Analytic Prediction of the Maximum Amplitude of Slender Wing Rock

L. E. Ericsson*
Lockheed Missiles & Space Company, Inc., Sunnyvale, California

Wing rock of slender delta wings is controlled by two vortical flow phenomena: asymmetric vortex shedding from the wing leading edges and breakdown of these leading-edge vortices. The asymmetric vortex shedding provides the mechanism driving the wing rock motion, and the vortex breakdown or burst provides the mechanism limiting the amplitude of the wing rock. Simple analytic means are presented by which the maximum wing rock amplitude measured experimentally can be predicted.

Nomenclature

A = aspect ratio, $= b^2/S$
b = wingspan
c_0 = root chord
f = frequency of oscillation
ℓ = rolling moment; coefficient $C_\ell = \ell/(\rho_\infty U_\infty^2/2)Sb$
N = normal force; coefficient $C_N = N/(\rho_\infty U_\infty^2/2)S$
Re = Reynolds number based on c_0 and freestream conditions
s = local semispan
S = reference area (= projected wing area)
t = time
Δt = time lag
T = oscillation period
U = velocity
$\bar{U}$ = convection velocity
x = chordwise distance from apex
y = spanwise distance from symmetry plane
α = angle of attack
β = angle of sideslip
Δ = increment or amplitude
Γ = vortex strength
η = dimensionless y coordinate, $= y/s$
θ = angular perturbation in pitch
θ_A = apex half-angle
θ_{LE} = complimentary angle to the leading-edge sweep, $= \pi/2 - \Lambda$
Λ = leading-edge sweep angle
ξ = dimensionless x coordinate, $= x/c_0$
ρ = air density
ϕ = roll angle
ω = angular frequency $= 2\pi f$
$\bar{\omega}$ = reduced frequency, $= \omega c_0/U_\infty$

Subscripts

a = attached flow
A = apex
C = critical
eff = effective
H = hysteresis
LE = leading edge
max = maximum
V = vortex
VA = vortex asymmetry
WR = wing rock
0 = initial or time-average value
1,2 = numbering subscripts
∞ = freestream conditions

Superscript

$(\bar{})$ = integrated mean values, e.g., centroid of aerodynamic loads

Differential Symbols

$\dot{\phi}$ = $\partial\phi/\partial t$
$C_{\ell\beta}$ = $\partial C_\ell/\partial\beta$
$C_{\ell\dot{\phi}}$ = $\partial C_\ell/\partial(b\dot{\phi}/2U_\infty)$

Introduction

EVER since Nguyen et al.[1] presented the results for an 80-deg delta wing (Fig. 1). the slender wing rock phenomenon has received considerable attention.[2-7] This paper offers a simple analytic method for prediction of the maximum slender wing rock amplitude. The asymmetric vortex-induced effect on the rolling moment is determined theoretically by extension of previously developed analytic means[8,9]—not experimentally, as was the case in Ref. 5.

Analytic Approach

It was discussed in Ref 5 how the loss of vortex-induced lift due to vortex asymmetry, in combination with the time lag associated with the change in vortex-induced lift, could explain the slender wing rock phenomenon. From the flow-visualization results[10] in Fig. 2, it is obvious that the lifted-off vortex

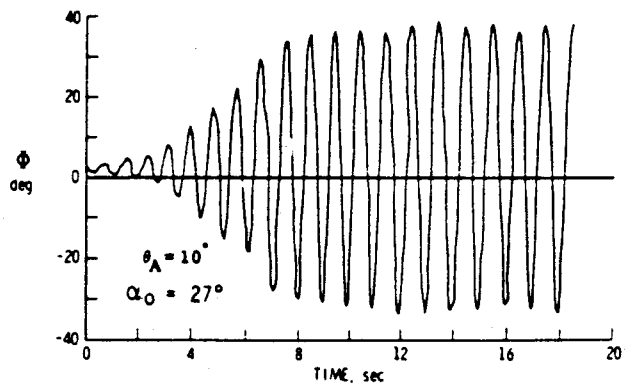

Fig. 1 Time history of wing rock at $\alpha = 27$ deg of an 80-deg delta wing.[1]

Presented as Paper 87-2496 at the AIAA Atmospheric Flight Mechanics Conference, Monterey, CA, Aug. 17–19, 1987; received Aug. 31, 1987; revision received Feb. 12, 1988.

*Senior Consulting Engineer. Fellow AIAA.

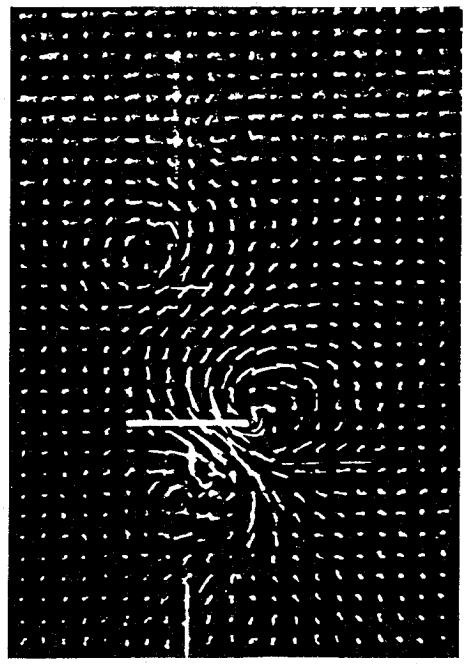

Fig. 2 Tuft-grid flow picture of asymmetric vortex shedding from an 86.5 deg delta wing at $\alpha = 25$ deg.[10]

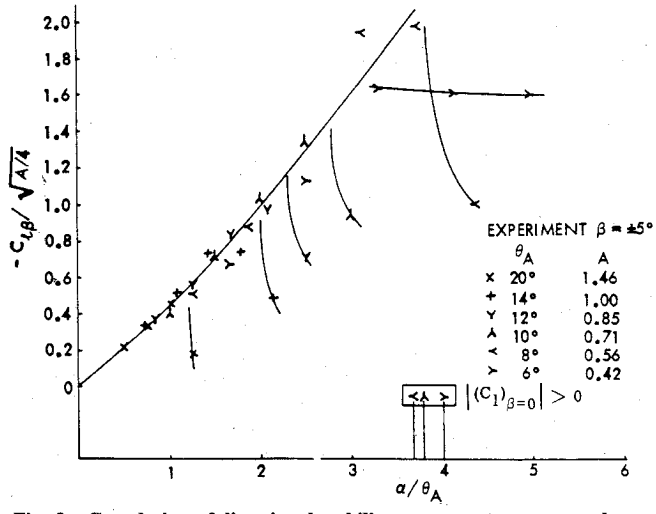

Fig. 3 Correlation of directional stability, vortex asymmetry, and vortex burst for slender, sharp-edged delta wings.

cannot induce any significant lift on the delta wing. As was shown in Refs. 8 and 9 and is demonstrated by Fig. 3, the delta wing aerodynamics are a function of α/θ_{LE}, or $\tan\alpha/\tan\theta_{LE}$ for higher values of α and θ_{LE}. The boundary for vortex asymmetry determined experimentally[11] (Fig. 4) obeys the following relationship:

$$\frac{\tan\alpha_{VA}}{\tan\theta_{LE}} = \sqrt{3 + 66/\theta^{\circ}_{LE}} \tag{1}$$

Analysis

The analytic theory developed in Refs. 8 and 9 will be applied to the analysis in Ref. 5 in order to develop analytic means for prediction of the maximum wing rock amplitude of slender delta wings. Based on the experimental results[10] in Fig. 2, it is assumed that the vortex-induced rolling moment contribution is lost completely for the lifted-off vortex.

According to Ref. 11, on each wing half of a sharp-edged delta wing, the leading-edge vortex generates the total normal force C_{NV}, where

$$C_{NV} = (\pi/2)\sin^2\alpha \tag{2}$$

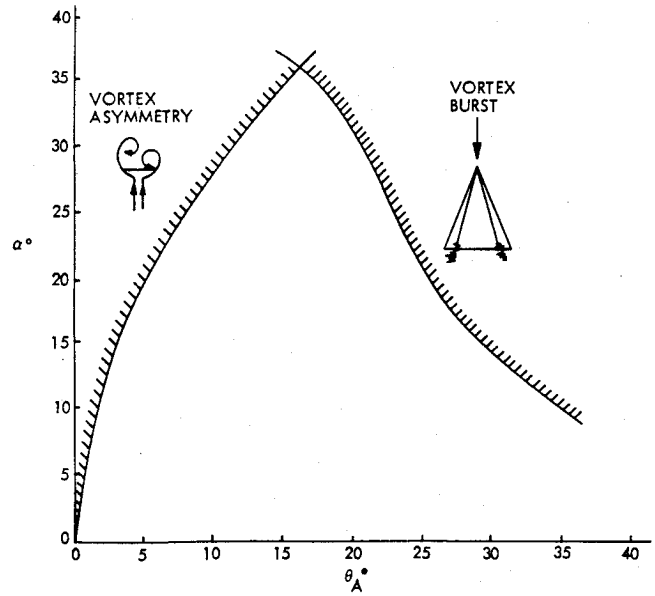

Fig. 4 Boundaries for vortex symmetry and vortex burst.[11]

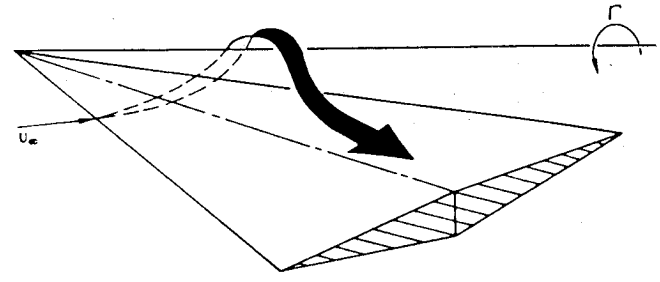

Fig. 5 Entrainment effect of leading-edge vortex.[8]

It was shown in Ref. 8 that 30% of this vortex-induced normal force is generated by the entrainment effect of the leading-edge vortex (Fig. 5). The two different vortex-induced load components have different longitudinal and spanwise aerodynamic centers, $\bar{\xi}$ and $\bar{\eta}$, respectively. The entrainment effect generates a load with the same aerodynamic center as the attached-flow loading[5,9]

$$\bar{\xi}_{0.3V} = \bar{\xi}_a = 0.64(1 - \bar{\eta}_a \sin^2\theta_{LE}) \tag{3a}$$

$$\bar{\eta}_{0.3V} = \bar{\eta}_a = 4/3\pi \tag{3b}$$

The remaining 70% of the vortex-induced normal force has the following aerodynamic center[5,9]:

$$\bar{\xi}_{0.7V} = 0.56(1 - \bar{\eta}_{0.7V}) \tag{4a}$$

$$\bar{\eta}_{0.7V} = 0.56 + 0.36/(1.75 + \tan\alpha/\tan\theta_{LE}) \tag{4b}$$

Combining Eqs. (2–4) gives the following vortex-induced rolling moment coefficient for the wing half on which the leading-edge vortex has not been lifted off.

$$C_{\ell V} = C_{NV}(0.7\,\bar{\xi}_{0.7V}\,\bar{\eta}_{0.7V} + 0.3\,\bar{\xi}_a\,\bar{\eta}_a) \tag{5}$$

Following Ref. 5, the wing rock analysis then can proceed as follows. At high angles of attack, where asymmetric vortex liftoff occurs, the rolling moment changes discontinuously at a critical roll angle ϕ_C

$$C_\ell = \begin{cases} C_{\ell_1}(\phi): & |\phi| \le \phi_C \\ C_{\ell_2}(\phi): & |\phi| > \phi_C + \Delta\phi_H \end{cases} \tag{6}$$

where $\Delta\phi_H$ represents any occurring hysteresis. For simplicity, it will be assumed that $\Delta\phi_H = 0$ in the following analysis.

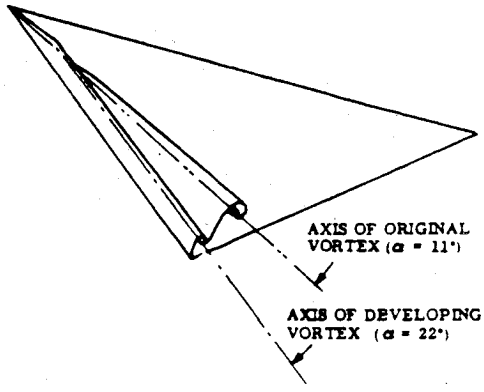

Fig. 6 Leading-edge vortex formation on a slender delta wing.[12]

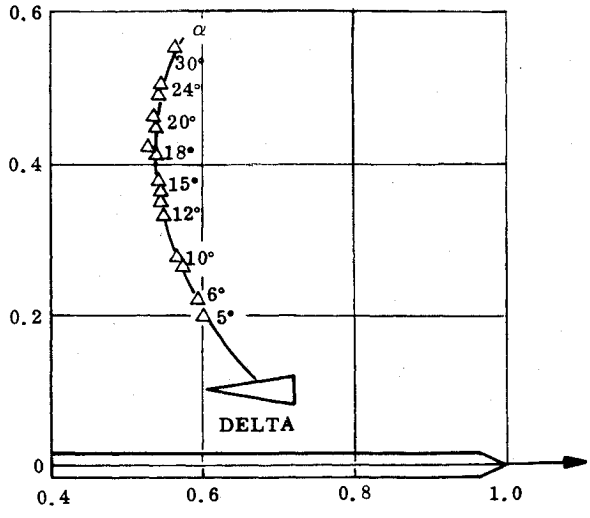

Fig. 7 Effect of α on leading-edge vortex location.[13]

The rolling moments $C_{\ell 1}(\phi)$ and $C_{\ell 2}(\phi)$ can be expressed in the following form:

$$C_{\ell_1}(\phi) = C_\ell(\alpha) + C_{\ell\phi_1}\phi + C_{\ell\dot{\phi}_1}\frac{b\dot{\phi}}{2U^\infty} \tag{7a}$$

$$C_{\ell_1}(\phi) = C_\ell(\alpha) + C_{\ell\phi_1} - C_{\ell\phi_2})\phi_C + C_{\ell\phi_2}\phi + \Delta C_\ell \frac{\phi}{|\phi|} + C_{\ell\dot{\phi}_2}\frac{b\dot{\phi}}{2U_\infty} \tag{7b}$$

The vortex-induced rolling moment, acting at the load center $\bar{x} = c_0\bar{\xi}$, is determined by the roll angle at apex at a time increment Δt earlier, where Δt is the time required to convect the vortex change from the apex to x (Fig. 6). That is, for sinusoidal oscillations, $\phi = \Delta\phi \sin \omega t$.

$$\phi_A = \Delta\phi \sin(\omega t - \omega\Delta t) = \Delta\phi \sin(\psi - \Delta\psi) \tag{8a}$$

$$\Delta\psi = \omega\Delta t = \omega c_0\bar{\xi}/\bar{U}_V = \frac{U_\infty}{\bar{U}_V}\bar{\xi}\bar{\omega} \tag{8b}$$

For roll oscillations through the discontinuity ϕ_C, an effective damping derivative $C_{\bar{\ell}\dot{\phi}}$ can be determined by considering the energy dissipation through one cycle of oscillation.

$$\int_{t_0}^{t_0+T} C_\ell(t)\,\mathrm{d}\phi = \int_{t_0}^{t_0+T} C_\ell(t)\dot{\phi}\,\mathrm{d}t = \int_{t_0}^{t_0+T} C_{\bar{\ell}\dot{\phi}}\frac{b\dot{\phi}}{2U_\infty}\dot{\phi}\,\mathrm{d}t \tag{9}$$

That is,

$$C_{\bar{\ell}\dot{\phi}} = \int_{t_0}^{t_0+T} C_\ell(t)\dot{\phi}\,\mathrm{d}t \Big/ \frac{b}{2U_\infty}\int_{t_0}^{t_0+T}\dot{\phi}^2\,\mathrm{d}t \tag{10}$$

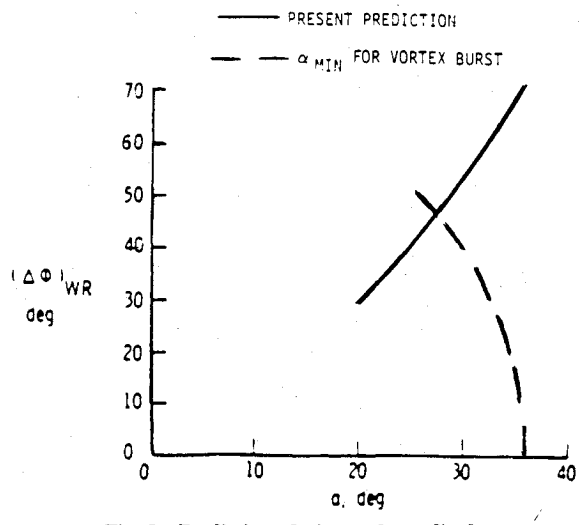

Fig. 8 Prediction of wing rock amplitude.

Or, with $\phi = \Delta\phi \sin\psi$, where $\psi = \omega t$,

$$C_{\bar{\ell}\dot{\phi}} = \frac{1}{\pi\,\Delta\phi}\frac{1}{(b\omega/2U_\infty)}\int_{\psi_0}^{\psi_0+2\pi} C_\ell(\psi)\,\mathrm{d}\psi \tag{11}$$

One can combine Eqs. (7), (8), and (11) to obtain the following definition of $C_{\bar{\ell}\dot{\phi}}$:

$$C_{\bar{\ell}\dot{\phi}} = \frac{2}{\pi\,\Delta\phi}\frac{1}{(b\omega/2U_\infty)}\left\{\int_{\Delta\psi}^{\Delta\psi+\psi_1} C_{\ell_1}\cos\psi\,\mathrm{d}\psi + \int_{\Delta\psi+\psi_1}^{\pi+\Delta\psi-\psi_1} C_{\ell_2}\cos\psi\,\mathrm{d}\psi + \int_{\pi+\Delta\psi-\psi_1}^{\pi+\Delta\psi} C_{\ell_1}\cos\psi\,\mathrm{d}\psi\right\}$$

$$= C_{\ell\phi_2} - \frac{4}{\pi}\frac{C_{\ell_V}}{\Delta\phi}\frac{\sin(\bar{\omega}\bar{\xi}U_\infty/\bar{U}_v)}{b\bar{\omega}/2c_0} + \frac{2}{\pi}(C_{\ell\phi_1} - C_{\ell\phi_2}) \times\left[\sin^{-1}\left(\frac{\phi_C}{\Delta\phi}\right) - \left(\frac{\phi_C}{\Delta\phi}\right)\sqrt{1-\left(\frac{\phi_C}{\Delta\phi}\right)^2}\cos(2\Delta\psi)\right] \tag{12}$$

According to the discussion in Ref. 5, the maximum amplitude of the wing rock is rather insensitive to Φ_C, decreasing slightly with increasing Φ_C. Thus, a slightly conservative value of the wing rock maximum amplitude is obtained by setting $\Phi_C = 0$ in Eq. (12), thereby eliminating the third term. Thus, the limit-cycle amplitude, defined by setting $C_{\bar{\ell}\dot{\phi}} = 0$ in Eq. (12), becomes

$$\Delta\phi_{WR} = \frac{C_{\ell_V}}{C_{\ell\dot{\phi}_2}}\frac{\sin(\bar{\omega}\bar{\xi}U_\infty/\bar{U}_v)}{\bar{\omega}\tan\theta_{LE}} \tag{13}$$

For the 80-deg delta wing tested by Nguyen et al.[1], the reduced frequency was $\bar{\omega} = 1.12$, and a value $C_{\ell\dot{\phi}_2} \approx -0.4$ was indicated by the experimental results. As discussed in Ref. 8, the tests by Lambourne et al.[12] indicated a value of $U_\infty/\bar{U}_V = 0.75$ in regard to the convection of the vortex strength and its height above the wing surface, whereas a value of $U_\infty/\bar{U}_V = 1.00$ was indicated for its lateral movement across the wing surface. For the high angles of attack where vortex asymmetry occurs, experimental results[13] show that the lateral position varies little with further α changes (Fig. 7). Thus, the value $U_\infty/\bar{U}_V = 0.75$ should be used in Eqs. (3). Combining Eqs. (2–5) and (13) gives the predicted wing rock amplitude shown in Fig. 8.

Also shown in Fig. 8 is the maximum effective angle of attack for which vortex burst does not occur. α_{eff} for the rocking wing is obtained from Ref. 5 as follows:

$$\alpha_{eff} = \arctan(\tan\alpha_0\cos\phi) \tag{14}$$

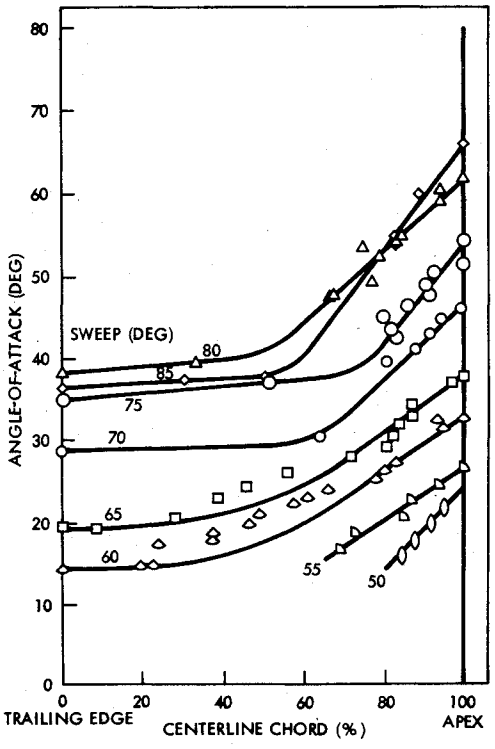

Fig. 9 Vortex breakdown position on sharp-edged delta wings.[15]

where α_0 is the mean angle of attack. From the compilation by Cunningham,[14] one finds that the angle of attack for vortex burst (at $\beta = \phi = 0$) approaches $\alpha = 40$ deg when the leading-edge sweep approaches $\Lambda = 90$ deg. Using these results to compute $\alpha_{\text{eff}} = \alpha_{\text{burst}}$ for $\alpha_0 = 36$ deg (burst occurs at $\beta = \phi = 0$ when $\alpha_0 = 36$ deg) gives the burst boundary shown in Fig. 8. The present prediction is valid only below this boundary.

When burst starts occurring on the delta wing, its effect is almost discontinuous for the sweep angles causing wing rock ($\Lambda > 74$ deg in Fig. 4), according to experimental results[15] (Fig. 9). As the effect of vortex burst is damping in regard to the wing rock, as was demonstrated in Ref. 5 and has been observed experimentally,[3] one can expect the burst to cause a sudden halt of the increase of the wing rock amplitude. Thus, the intersection between the two curves in Fig. 8 should indicate the maximum possible wing rock amplitude.

Adding the experimental results from Refs. 1 and 2 to the prediction in Fig. 8 gives the results shown in Fig. 10. The intersection point appears indeed to denote the maximum possible wing rock amplitude. As could be expected, the assumption of total loss of the suction load from the lifted-off vortex gives a conservatively high value of the wing rock amplitude.

The tested Reynolds number effect at $\alpha = 35$ deg on the wing rock amplitude (Fig. 11) is indicated in Fig. 10. It can be seen that the difference in Reynolds number could indeed explain the difference between the two experiments shown in Fig. 10. Vortex breakdown has shown great sensitivity not only to the Reynolds number but also to the similar effects of wind-tunnel turbulence and (possibly) surface roughness[16] (Fig. 12).

Combining the results in Figs. 4 and 10, one can see that no wing rock is likely to occur for $\theta_A > 16$ deg, i.e., $\Lambda < 74$ deg. Thus, the claim made in Ref. 7 that the presented analysis, contrary to the one in Ref. 5, could predict wing rock for leading-edge sweep angles larger than 74 deg is of little practical value. Going back to Fig. 4, it is indicated that, for $\theta_A = 10$ deg, i.e., $\Lambda = 80$ deg, spontaneous wing rock would only occur at $\alpha \geq 27$ deg, as was also observed by Nguyen et al.[1] However, if wing rock is started by some disturbance or ϕ perturbation, wing rock can result at as low an angle of attack as $\alpha = 20$ deg, as was demonstrated by Levin and Katz.[2]

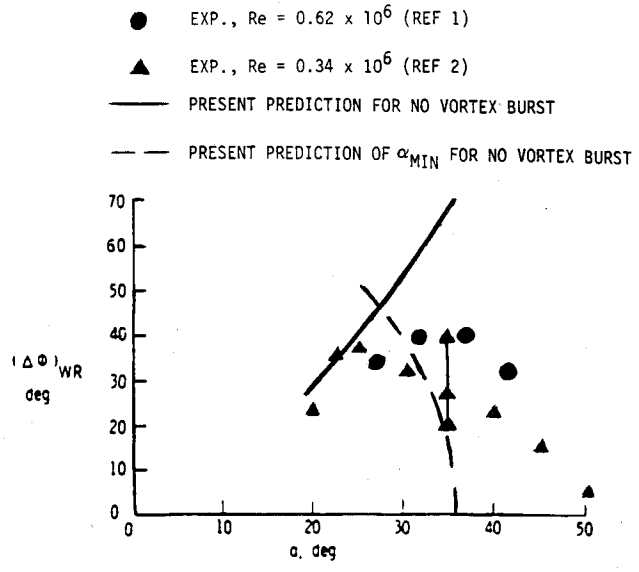

Fig. 10 Comparison between predicted and measured wing rock amplitude.

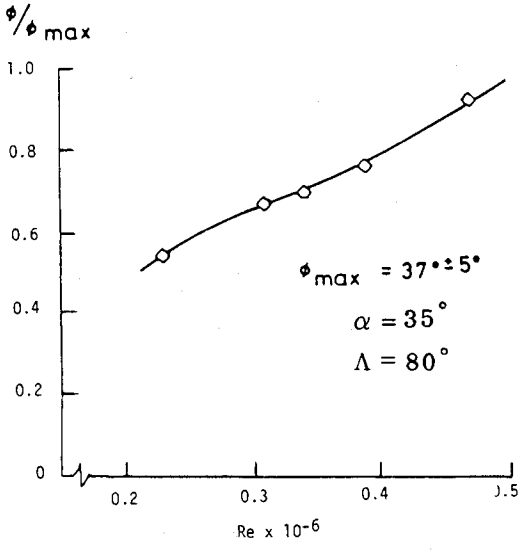

Fig. 11 Effect of Reynolds number on wing rock amplitude.

In the analysis in Ref. 5, the experimentally observed value of $C_{\ell V}$ was used in the analysis, giving a constant value $(\Delta\phi)_{\text{WR}} \approx 36$ deg over the complete α range 30 deg $\leq$ 40 deg, which was in excellent agreement with the experimental results obtained by Nguyen et al.[1] The reason for this is, of course, that the effect of vortex burst was already included in the used experimental value of $C_{\ell V}$.

The present analysis shows conclusively that vortex burst is the flow mechanism limiting the amplitude of wing rock at increasing angle of attack. Because of the complexity of the burst mechanism, leading-edge vortex burst cannot be predicted even in the static case (Fig. 12 illustrates some of the difficulties), much less in the dynamic case of wing rock. Existing theories[4-7] simply ignore the presence of vortex burst, in spite of the fact that experiments[1,2] (Fig. 13) show its presence. Because of the discontinuous nature of the burst appearance (Fig. 9), the wing rock amplitude reached at that time, obtained as the intersection between the two predicted curves in Fig. 8, should be the maximum possible amplitude. As this prediction is supported by the available experimental results[1,2] (Fig. 10), the presented analytic theory should be a valuable preliminary design tool.

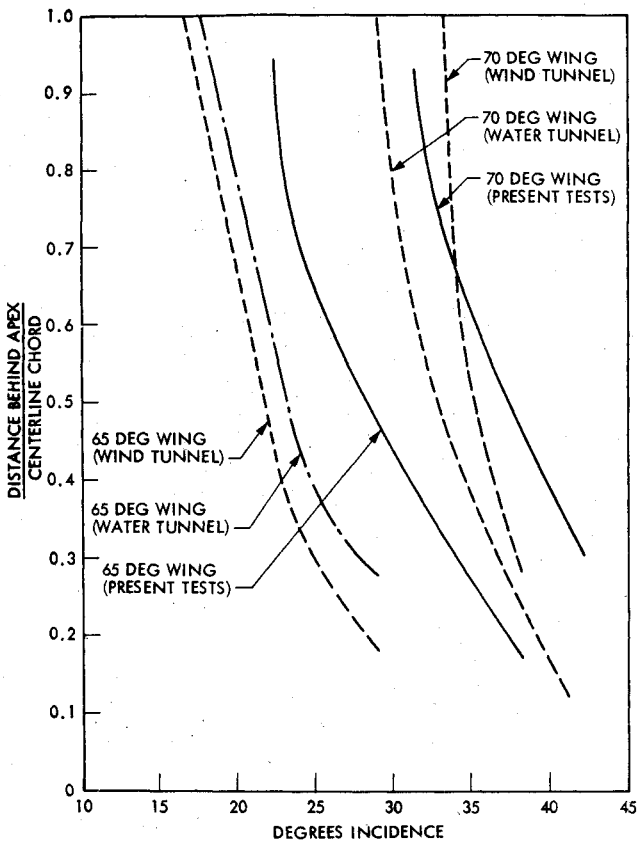

Fig. 12 Comparison of vortex breakdown measured in different wind tunnels and in a water tunnel.[16]

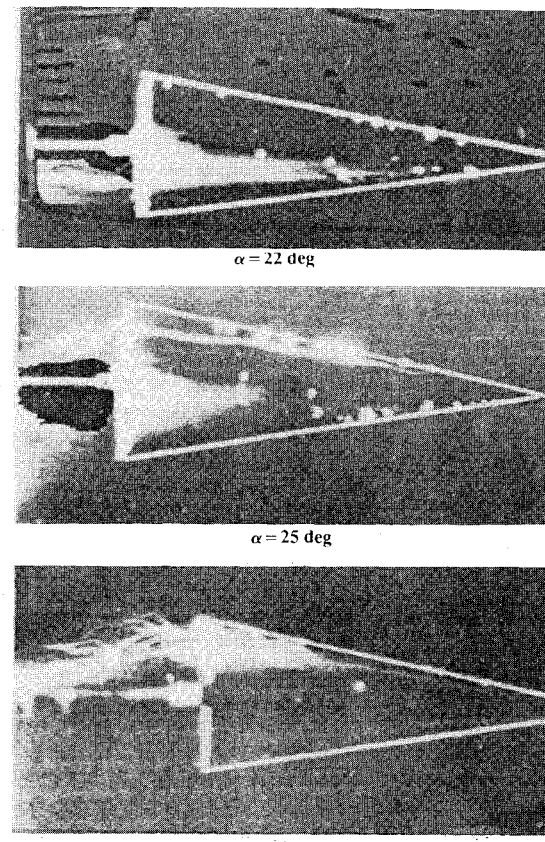

Fig. 13 Most forward vortex burst position during wing rock.[2]

Conclusions

Further analysis of the slender wing rock phenomenon has shown that vortex asymmetry drives the motion, and the wing rock amplitude is limited only by the vortex burst phenomenon. No analysis is valid that does not recognize the importance of both flow phenomena. Because of the complexity of especially the vortex burst phenomenon, it will be some time before slender wing rock can be predicted by purely theoretical means. In the meantime, the presented simplified analysis presents the vehicle designer with a tool for prediction of the maximum possible wing rock amplitude.

References

[1]Nguyen, L. E., Yip, L. P., and Chambers, J. R., "Self Induced Wing Rock of Slender Delta Wings," AIAA Paper 81-1883, Aug. 1981.

[2]Levin, D. and Katz, J., "Dynamic Load Measurements with Delta Wings Undergoing Self-Induced Roll-Oscillations," *Journal of Aircraft*, Vol. 21, Jan. 1984, pp. 30–36.

[3]Katz, J. and Levin, D., "Self-Induced Roll Oscillations Measured on a Delta Wing/Canard Configuration," *Journal of Aircraft*, Vol. 23, Nov. 1986, pp. 801–807.

[4]Konstadinopoulus, P., Mook, D. T., and Nayfeh, A. H., "Numerical Simulation of the Subsonic Wing Rock Phenomenon," AIAA Paper 83-2115, Aug. 1983.

[5]Ericsson, L. E., "The Fluid Mechanics of Slender Wing Rock," *Journal of Aircraft*, Vol. 21, May 1984, pp. 322–328.

[6]Konstadinopoulus, P., Mook, D. T. and Nayfeh, A. H., "Numerical Rock of Slender Delta Wings," *Journal of Aircraft*, Vol. 22, Oct. 1985, pp. 920–924.

[7]Hsu, C. H. and Lan, C. E., "Theory of Wing Rock," AIAA Paper 85-0199, Jan. 1985.

[8]Ericsson, L. E. and Reding, J. P., "Unsteady Aerodynamics of Slender Delta Wings at Large Angles of Attack," *Journal of Aircraft*, Vol. 12, Sept. 1975, pp. 721–729.

[9]Ericsson, L. E. and Reding, J. P., "Approximate Nonlinear Slender Wing Aerodynamics," *Journal of Aircraft*, Vol. 14, Oct. 1977, pp. 1197–1200.

[10]Bird, J. D., "Tuft-Grid Surveys at Low Speeds for Delta Wings," NASA TND-5045, Feb. 1969.

[11]Polhamus, E. C., "Predictions of Vortex-Lift Characteristics by a Leading-Edge-Suction Analogy," *Journal of Aircraft*, Vol. 8, April 1971, pp. 193–199.

[12]Lambourne, N. C., Bryer, D. W., and Maybrey, J. F. M., "The Behavior of the Leading-Edge Vortices over a Delta Wing Following a Sudden Change of Incidence," Aeronautical Research Council, England, UK, R & M 3645, March 1969.

[13]Werlé, H., "Vortices from Very Slender Wings," *La Recherche Aérospatiale*, No. 109, Nov.–Dec. 1965, pp. 1–12.

[14]Cunningham, A. M., Jr., "Vortex Flow Hysteresis," *Vortex Flow Aerodynamics*, Vol. 1, NASA CP 2416, 1986.

[15]Wendtz, W. H. and Kohlman, D. L., "Vortex Breakdown on Slender Sharp-Edged Delta Wings," AIAA Paper 69-778, July 1969.

[16]Earnshaw, P. B., "Measurements of Vortex Breakdown Position at Low Speed on a Series of Sharp-Edged Symmetrical Models," Aeronautical Research Council, England, UK, CP 828, 1965.